

Stability Criteria for Robot Compliant Maneuvers

H. Kazerooni

T. I. Tsay

Mechanical Engineering Department
University of Minnesota
Minneapolis, Minnesota, 55455

Abstract

The work presented here is a nonlinear approach for the stability analysis of robot manipulators in constrained maneuvers. Stability of the environment and the manipulator taken as a whole has been investigated, and a bound for stable manipulation has been derived. We show that for stability of the robot, there must be some initial compliancy either in the robot or in the environment. The general stability condition has been extended to the particular case where the environment is very rigid in comparison with the robot stiffness. The stability analysis has been investigated using unstructured models for the dynamic behavior of the robot manipulator and the environment. This unified approach of modeling robot dynamics is expressed in terms of sensitivity functions as opposed to the Lagrangian approach. It allows us to incorporate the dynamic behavior of all the elements of a robot manipulator (i.e. actuators, sensors and the structural compliance of the links) in addition to the rigid body dynamics.

Nomenclature

d	vector ¹ of the external force on the robot endpoint
e	input trajectory vector
E	environment dynamics
f	vector of the contact force, $\{f_1, f_2, \dots, f_n\}^T$
f_{∞}, U_{∞}	the limiting value of the contact force and robot position for rigid environment
G	robot dynamics with positioning controller
H	compensator operating on the contact force, f
I_n	identity matrix
$J_s^2 + D_s + K$	environment impedance in the linear domain
r	input-command vector
n	degrees of the freedom of the robot $n \leq 6$
S	robot manipulator sensitivity (1/stiffness)
T	positive scalar
V	the forward loop mapping from e to f in Figure 5.
x	vector of the environment deflection
y	vector of the robot endpoint position
x_0	vector of the environment position before contact
θ	vector of the joint angles of the robot
$\epsilon_0, \epsilon_d, \mu, \gamma$	positive scalars
ω_0	frequency range of operation (bandwidth)
α_1, β_1, ν	positive scalars

1. Introduction

Most assembly operations and manufacturing tasks require mechanical interactions with the environment or with the object being manipulated, along with "fast" motion in free and unconstrained space. In constrained maneuvers, the interaction force² must be accommodated rather than resisted. Two methods have been suggested for development of compliant motion. The first approach is aimed at controlling force and

position in a nonconflicting way (10,11,12,18). In this method, force is commanded along those directions constrained by the environment, while position is commanded along those directions in which the manipulator is unconstrained and free to move. The second approach is focused on developing a relationship between the interaction forces and the manipulator position (1,3,4,7,13). By controlling the manipulator position and specifying its relationship with the interaction forces, a designer can ensure that the manipulator will be able to maneuver in a constrained space while maintaining appropriate contact forces. This paper describes an analysis on the stability of the robot and environment taken as a whole when the second method is employed to control the robot compliancy.

We start with modeling the robot and the environment with unstructured dynamic models. To arrive at a general stability criteria, we avoid using structured dynamic models such as first or second order transfer functions as general representations of the dynamic behavior of the components of the robot (such as actuators). Using the unstructured models for the robot and environment, we analyze the stability of the robot and environment via the Small Gain Theorem and Nyquist Criterion. We show that the stability criteria achieved via the Nyquist method is a subclass of condition given by the Small Gain Theorem. For a particular application, one can replace the unstructured dynamic models with known models and then a tighter condition can be achieved. The stability criterion reveals that there must be some initial compliancy either in the robot or in the environment. The initial compliancy in the robot can be obtained by a passive compliant element such as an RCC (Remote Center Compliance) or compliancy within the positioning feedback. Practitioners always observed that the system of a robot and a stiff environment can always be stabilized when a compliant element (e.g. piece of rubber or an RCC) is installed between the robot and environment. The stability criterion also shows that no compensator can be found to stabilize the interaction of the ideal positioning system (very rigid tracking robot) with an infinitely rigid environment. In this case the robot and environment both resemble ideal sources of flow (defined in bond graph theory) and they do not physically complement each other.

2. Dynamic Model of the Robot

In this section, a general approach will be developed to describe the dynamic behavior of a large class of industrial and research robot manipulators having positioning (tracking) controllers. The fact that most industrial manipulators already have some kind of positioning controller is the motivation behind our approach. Also, a number of methodologies exist for the development of robust positioning controllers for direct and

¹ All vectors in this paper are $n \times 1$ vectors.

² In this article, "force" implies force and torque and "position" implies position and orientation.

non-direct robot manipulators (14,17).

In general, the endpoint position of a robot manipulator that has a positioning controller is a dynamic function of its input trajectory vector, e , and the external force, d . Let G and S be two functions that describe the robot endpoint position, y , in a global coordinate frame.³ (d is measured in the global coordinate frame also.)

$$y = G(e) + S(d) \quad (1)$$

The motion of the robot endpoint in response to imposed forces, d , is caused by either structural compliance in the robot⁴ or by the compliance of the positioning controller. Robot with tracking controllers are not infinitely stiff in response to external forces (also called disturbances). Even though the positioning controllers of robots are usually designed to follow the trajectory commands and reject disturbances, the robot endpoint will move somewhat in response to imposed forces on it. S is called the sensitivity function and it maps the external forces to the robot position. For a robot with a "good" positioning controller, S is a mapping with small gain. No assumption on the internal structures of $G(e)$ and $S(d)$ are made. Figure 1 shows the nature of the mapping in equation 1.

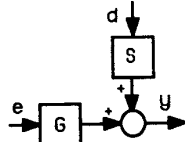


Figure 1: The Dynamics of the Robot. All the operators of the block diagrams are unspecified and may be transfer function matrices or time domain input-output relationships.

Figure 2 shows one possible example of internal structure of the model represented by equation 1. The robot open loop dynamic equation is $M(\theta)\ddot{\theta} + C(\theta, \dot{\theta}) + G_r(\theta) = \tau + J_0^T d$ where $M(\theta)$, $C(\theta, \dot{\theta})$, $G_r(\theta)$ and J_0 are the inertia matrix, coriolis, gravity forces and the Jacobian. With the help of two mappings, T_1 and T_2 , we define θ_d and θ as the desired position and the actual position of the robot in the joint coordinate frame. $P1$ and $P2$ are computer programs that calculate the best estimated values of nonlinear terms in robot dynamics. K_p and K_v are appropriate position and velocity gains to stabilize the system (17). The system in Figure 2 with two inputs (e and d), and one output, y , can be represented by block diagram of Figure 1. Note that equation 1 is not necessarily restricted to be composed of the elements of the block diagram of Figure 2; the block diagram of Figure 2 is given here as an example to show how one can actually model a robot with equation 1. Also note that the model given by equation 1 is not meant to be valid for controller design; it is only for the purpose of stability analysis.

Equation 1 represents an input/output functional relationship. This unified approach of modeling allows us to incorporate the dynamic behavior of all the elements of the robot. We believe that there may be enough components in the robot itself that rigid body dynamics (as given in Figure 2) is not sufficient for modeling. In fact, in many industrial hydraulic robots, the actuators and the servovalves dynamics dominate the

³The assumption that linear superposition (in equation 1) holds for the effects of d and e is useful in understanding the nature of the interaction between the robot and the environment. This interaction is in a feedback form and will be clarified with the help of Figure 3. We will note in Section 4 that the results of the nonlinear analysis do not depend on this assumption, and one can extend the obtained results to cover the case when $G(e)$ and $S(d)$ do not superimpose.

⁴In a simple example, if a Remote Center Compliance (RCC) with a linear dynamic behavior is installed at the endpoint of the robot, then S is equal to the reciprocal of stiffness (impedance in the dynamic sense) of the RCC.

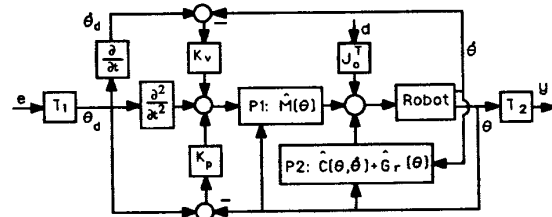


Figure 2: An example to develop positioning controller for a robot manipulator with rigid body dynamics. $\hat{M}(\theta)$, $\hat{C}(\theta, \dot{\theta})$ and $\hat{G}_r(\theta)$ are the estimated values (17).

total dynamic behavior of the robots. We try to avoid using structured dynamic models such as first or second order transfer functions as general representations of the dynamic behavior of the components of the robot (e.g. servovalves in the hydraulic robots and the gear stiffness in the non-direct drive systems). Throughout this paper we assume the robot dynamic behavior is given by equation 1 where $G(e)$ and $S(d)$ can be computed experimentally or analytically from the closed loop block diagram similar to the one given in Figure 2. A robot with good tracking capability has a small gain for S (rejects all the forces) while a robot with a weak tracking capability has a large gain for S . In fact, an open loop robot -which has the weakest tracking capability- can be modeled with the largest gain on S . If we define an open loop robot as a system with very small feedback gain (K_p and $K_v \rightarrow 0$ in the case of Figure 2) then equation 1 -with a large gain for S - can be used to model the open loop robots also. Therefore we define $G(e)$ and $S(d)$ as stable, nonlinear operators in L_p -space to represent the dynamic behavior of not only the closed loop robots but also the open loop (in the sense of above definition) robots. $G(e)$ and $S(d)$ are such that $G: L_p^n \rightarrow L_p^n$, $S: L_p^n \rightarrow L_p^n$ and also there exist constants α_1 , β_1 , α_2 , and β_2 such that $\|G(e)\|_p < \alpha_1 \|e\|_p + \beta_1$ and $\|S(d)\|_p < \alpha_2 \|d\|_p + \beta_2$. α_2 is called the gain of operator S .

A similar modeling method can be given for analysis of the linearly treated robots⁵. The transfer function matrices, G and S in equation 2 are defined to describe the dynamic behavior of a linearly treated robot manipulator with positioning controller.

$$y(j\omega) = G(j\omega)e(j\omega) + S(j\omega)d(j\omega) \quad (2)$$

In equation 2, S is called the sensitivity transfer function matrix and it maps the external forces to the end point position. $G(j\omega)$ is the closed loop transfer function matrix that maps the input trajectory vector, e , to the robot position, y . For a robot with a "good" positioning controller, within the closed loop bandwidth $S(j\omega)$ is "small" in the singular value sense,⁶ while $G(j\omega)$ is approximately a unity matrix. If we define an open loop linearly treated robot as a system with very small feedback gain then equation 2 -with a "large" S - can be used to model the open loop robots also.

3. Dynamic Behavior of the Environment

The environment can be very "soft" or very "stiff". We do not restrain ourselves to any geometry or to any

⁵Throughout this paper, for the benefit of clarity, we develop the frequency domain theory for linearly treated robots in parallel with the nonlinear analysis. The linear analysis is useful not only for analysis of robots with inherently linear dynamics, but also for robots with locally linearized dynamic behavior. In the latter case, the analysis is correct only in the neighborhood of the operating point.

⁶The maximum singular value of matrix A , $\sigma_{\max}(A)$ is defined as:

$$\sigma_{\max}(A) = \max \frac{|Az|}{|z|}$$

where z is a non-zero vector and $|\cdot|$ denotes the Euclidean norm.

structure. If one point on the environment is displaced as vector of x , with force vector, f , then the dynamic behavior of the environment is given by equation 3.

$$f = E(x) \quad (3)$$

If x_0 is the initial location of the point of contact on the environment before deformation occurs then, $x = y - x_0$. E is assumed to be stable in L_p -sense; $E: L_p^n \rightarrow L_p^n$ and $\|E(x)\|_p < \alpha_3 \|x\|_p + \beta_3$. Confining equation 3 to cover the linearly treated environment, equation 4 represents the dynamic behavior of the environment.

$$f(j\omega) = E(j\omega) x(j\omega) \quad (4)$$

$E(j\omega)$ is a transfer function matrix that maps the amplitude of the displacement vector, x to the amplitude of the contact force, f . Matrix E is a $n \times n$ transfer function matrix. E is a singular matrix when the robot interacts with the environment in only some directions. For example, in grinding a surface, the robot is constrained by the environment in the direction normal to the surface only. Readers can be convinced of the truth of equation 4 by analyzing the relationship of the force and displacement of a spring as a simple model of the environment. E resembles the stiffness of a spring. References 3 and 4 represent $(Js^2 + Ds + K)$ for E where J , D and K are symmetric matrices and $s = j\omega$ (8). J is the positive definite inertia matrix while C and K are the positive semi definite damping and the stiffness matrices respectively.

4. Dynamics of the Robot and Environment

Suppose a manipulator with dynamic equation 1 is in contact with an environment given by equation 3; then $f = -d$. Figure 3 shows the dynamics of the robot manipulator and the environment when they are in contact with each other. Note that in some applications, the robot will have only uni-directional force on the environment. For example, in the grinding a surface by a robot, the robot can only push the surface. If one considers positive f_1 for "pushing" and negative f_1 for "pulling", then in this class of manipulation, the robot manipulator and the environment are in contact with each other only along those directions where $f_1 > 0$ for $i=1, \dots, n$. In some applications such as screwing a bolt, the interaction force can be positive and negative. This means the robot can have clockwise and counter-clockwise interaction torque. The nonlinear discriminator block-diagram in Figure 3 is drawn with dashed-line to illustrate the above concept.

Using equations 1 and 3, equations 5 and 6 represent the entire dynamic behavior of the robot and environment.

$$y = G(e) + S(-f) \quad (5)$$

$$f = E(x) \quad \text{where } x = y - x_0 \quad (6)$$

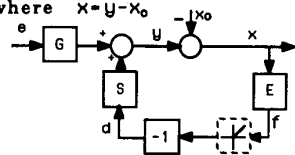


Figure 3: Interaction of the Robot with the Environment

If all the operators in Figure 3 are considered transfer function matrices, equations 7 and 8 can be obtained to represent the endpoint position and the contact force when $x_0 = 0$.

$$y = [I_n + SE]^{-1} G e \quad (7)$$

$$f = E [I_n + SE]^{-1} G e \quad (8)$$

To simplify the block diagram of Figure 3, we introduce a mapping from e to f .

$$f = V(e) \quad (9)$$

If all the operators in Figure 3 are transfer function matrices, then $V = E [I_n + SE]^{-1} G$. V is assumed to be a stable operator in

L_p -sense; therefore: $V: L_p^n \rightarrow L_p^n$ and also $\|V(e)\|_p < \alpha_4 \|e\|_p + \beta_4$. With this assumption, we basically claim that a robot with stable tracking controller remains stable when it is in contact with an environment. Note that one can still define V without assuming the superposition of effects of e and d in equation 5 (or equation 1).

5. The Architecture of the Closed-loop System

We propose the architecture of Figure 4 to develop compliancy for the robot. The compensator, H , is considered to operate on the contact force, f . The compensator output signal is being subtracted from the input command vector, r , resulting in the input trajectory vector, e , for the robot manipulator. The readers should be reminded that the robot in Figure 4 can be considered a weak tracking robot (open loop robot without any feedback on the position and velocity) when the gain of S is a large number.

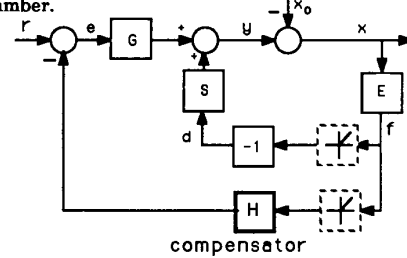


Figure 4: The Closed-loop System

There are two feedback loops in the system; the inner loop (which is the natural feedback loop), is the same as the one shown in Figure 3. This loop shows how the contact force affects the robot in a natural way when the robot is in contact with the environment. The outer feedback loop is the controlled feedback loop. If the robot and the environment are not in contact, then the dynamic behavior of the system reduces to the one represented by equation 1, which is a plain positioning system. When the robot and the environment are in contact, then the value of the contact force and the endpoint position of robot are given by f and y where the following equations are true:

$$y = G(e) + S(-f) \quad (10)$$

$$f = E(x) \quad \text{where } x = y - x_0 \quad (11)$$

$$e = r - H(f) \quad (12)$$

If the operators in equations 10, 11, and 12 are considered transfer function matrices, equations 13 and 14 can be obtained to represent the force and the robot end point position.

$$f = E [I_n + SE + GHE]^{-1} Gr \quad (13)$$

$$y = [I_n + SE + GHE]^{-1} Gr \quad (14)$$

The objective is to choose a class of compensators, H , to control the contact force with the input command r . By knowing S , G , E , and choosing H , one can shape the contact force. The value of H is the choice of designer and, depending on the task, it can have various values in different directions. A large value for H develops a compliant robot while a small H generates a stiff robot. Reference 7 describes a micro manipulator in which the compliancy in the system is shaped for metal removal application. Note that S and GH add in equation 14 to develop the total compliancy in the system. GH represents the electronic compliancy in the robot while S models the natural hardware compliancy (such as RCC or the robot structural compliancy) in the system⁷. Equation 13 also shows that a robot with good tracking capability (small gain for S) may generate a large contact force in a particular contact. One cannot choose arbitrarily large values for H ; the stability of the closed-loop system of Figure 4 must be guaranteed. The trade-off between the closed-loop stability and the size of H is investigated in Section 6.

When the robot is not in contact with the environment (i.e. the outer feedback loop in Figure 4 does not exist), the actual position of the robot endpoint is governed by equation 1. When the robot is in contact with the environment, then the contact force follows r according to equations 10, 11 and 12. The input command vector, r , is used differently for the two categories of maneuverings; as an input trajectory command in unconstrained space (equation 1) and as a command to control force in constrained space. We do not command any set-point for force as we do in admittance control (10,11,12,17). This method is called Impedance Control (1,3,4,7) because it accepts a position vector as input and it reflects a force vector as output. There is no hardware or software switch in the control system when the robot travels between unconstrained space and constrained space. The feedback loop on the contact force closes naturally when the robot encounters the environment.

6. Stability Analysis

The objective of this section is to arrive at a sufficient condition for stability of the system shown in Figure 4. This sufficient condition leads to the introduction of a class of compensators, H , that can be used to develop compliancy for the family of robot manipulators with dynamic behavior represented by equation 1. Using operator V defined by equation 9, the block diagram of Figure 5 is constructed as a simplified version of the block diagram of Figure 4. First we use the Small Gain Theorem to derive the general stability condition. Then, with the help of a corollary, we show the stability condition when H is chosen as a linear operator (transfer function matrix) while V is a nonlinear operator. Finally, if all the operators in Figure 4 are transfer function matrices, then the stability bound is shown by inequality 25. Section 7 is devoted to stability analysis of the linearly treated systems⁸, when the environment is infinitely rigid in comparison with the robot stiffness.

The following proposition (using the Small Gain Theorem references 15,16) states the stability condition of the closed-loop system shown in Figure 5.

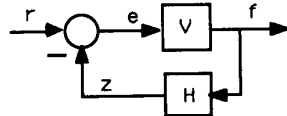


Figure 5: Simplified Version of Figure 4

If conditions I, II and III hold:

I. V is a L_p -stable operator, that is

$$a) \quad V(e): L_p^n \rightarrow L_p^n \quad (15)$$

$$b) \quad \|V(e)\|_p < \alpha_4 \|e\|_p + \beta_4 \quad (16)$$

II. H is chosen such that mapping $H(f)$ is L_p -stable, that is

$$a) \quad H(f): L_p^n \rightarrow L_p^n \quad (17)$$

$$b) \quad \|H(f)\|_p < \alpha_5 \|f\|_p + \beta_5 \quad (18)$$

⁷ Equation 13 can be rewritten as $f = (E^{-1} + S + GH)^{-1} Gr$. Note that the environment admittance (1/impedance in the linear domain), E^{-1} , the robot sensitivity (1/stiffness in the linear domain), S , and the electronic compliancy, GH , add together to form the total sensitivity of the system. If $H=0$, then only the admittance of the environment and the robot add together to form the compliancy for the system. By closing the loop via H , one can not only add to the total sensitivity but also shape the sensitivity of the system.

⁸ The stability analysis and the role of robot sensitivity and environment dynamics on size H are best shown by linear theory in equations 27-31. In particular, we confine our analysis to linear one-degree-of-freedom robot in equations 32 and 33 for better understanding the nature of the stability analysis.

III. and $\alpha_4 \alpha_5 < 1$ (19)

then the closed-loop system (Figure 5) is L_p -stable. This can be proved using the triangle inequality (6,15). Substituting for $\|f\|_p$ from inequality 16 into inequality 18 results in inequality 20. (Note that $f=V(e)$)

$$\|HV(e)\|_p < \alpha_4 \alpha_5 \|e\|_p + \alpha_5 \beta_4 + \beta_5 \quad (20)$$

$\alpha_4 \alpha_5$ in inequality 20 represents the gain of the loop mapping, $HV(e)$. The third stability condition requires that H be chosen such that the loop mapping, $HV(e)$, is linearly bounded with less than a unity slope. The following corollary develops a stability bound if H is selected as a linear transfer function matrix.

Corollary

The key parameter in the proposition is the size of $\alpha_4 \alpha_5$. According to the proposition, to guarantee the stability of the system, H must be chosen such that norm of $HV(e)$ is linearly bounded with a slope that is smaller than unity. If H is chosen as a linear operator (the impulse response) while all the other operators are still nonlinear, then:

$$\|HV(e)\|_p < \gamma \|V(e)\|_p \quad (21)$$

$$\text{where: } \gamma = \sigma_{\max}(N) \quad (22)$$

σ_{\max} indicates the maximum singular value, and N is a matrix whose ij th entry is $\|H_{ij}\|_1$. In other words, each member of N is the L_1 norm of each corresponding member of H . Considering inequality 16, inequality 21 can be rewritten as:

$$\|HV(e)\|_p < \gamma \|V(e)\|_p < \gamma \alpha_4 \|e\|_p + \gamma \beta_4 \quad (23)$$

Comparing inequality 23 with inequality 20, to guarantee the closed loop stability, $\gamma \alpha_4$ must be smaller than unity, or, equivalently:

$$\gamma < \frac{1}{\alpha_4} \quad (24)$$

To guarantee the stability of the closed loop system, H must be chosen such its "size" is smaller than the reciprocal of the "gain" of the forward loop mapping in Figure 5. Note that γ represents a "size" of H in the singular value sense.

When all the operators of Figure 5 are linear transfer function matrices one can use Multivariable Nyquist Criterion to arrive at the sufficient condition for stability of the closed loop system. This sufficient condition leads to the introduction of a class of transfer function matrices, H , that stabilize the family of linearly treated robot manipulators and environment using dynamic equations 2 and 4. Appendix A shows that the stability condition given by Nyquist Criterion is a subset of the condition given by the Small Gain Theorem. Using the results from references 6 and 9:

$$\sigma_{\max}(GHE) < \sigma_{\min}(SE + I_n) \quad \text{for all } \omega \in (0, \infty) \quad (25)$$

or a more conservative condition,

$$\sigma_{\max}(H) < \frac{1}{\sigma_{\max}\{E(I_n + SE)^{-1}G\}} \quad \text{for all } \omega \in (0, \infty) \quad (26)$$

Similar to the nonlinear case, H must be chosen such that its "size" is smaller than the reciprocal of the "size" of the forward loop mapping in Figure 6 to guarantee the stability of the closed loop system. Note that in equality 26 σ_{\max} represents a "size" of H in the singular value sense.

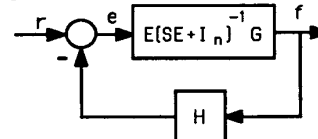


Figure 6: When all the operators are linear in Figure 5 are transfer function matrices, $V = E(SE + I_n)^{-1} G$.

Consider $n=1$ (one degree of freedom system) for more understanding about the stability criteria. The stability criteria when $n=1$ is given by inequality 27.

$$|HG| < |(S+1/E)| \quad \text{for all } \omega \in (0, \infty) \quad (27)$$

where $|\cdot|$ denotes the magnitude of a transfer function. Since in many cases $G \approx 1$ for all $0 < \omega < \omega_0$, then H must be chosen such that:

$$|H| < |(S+1/E)| \quad \text{for all } \omega \in (0, \omega_0) \quad (28)$$

Inequality 28 reveals some facts about the size of H . The smaller the sensitivity of the robot manipulator is, the smaller H must be chosen. Also from inequality 28, the more rigid the environment is, the smaller H must be chosen. In the "ideal case", no H can be found to allow a perfect positioning system ($S=0$) to interact with an infinitely rigid environment ($E=\infty$). In other words, for stability of the system shown in Figure 4, there must be some compliancy either in robot or in the environment. RCC, structural dynamics and the tracking controller stiffness form the compliancy on the robot. Section 7 gives more information about the effects of E on the stability region.

7. Stability for very rigid environment

In most manufacturing tasks, the endpoint of the robot manipulator is in contact with a very stiff environment. Robotic deburring and grinding are examples of practical tasks in which the robot is in contact with hard environment(5). It is easy to show that when the environment is very stiff, (E is very "large" in the singular value sense), the limiting value for the contact force and the endpoint position are given by equations 29 and 30 respectively:

$$f_\infty = (S+GH)^{-1}G r \quad (29)$$

$$y_\infty = 0 \quad (30)$$

Since $G \approx I_n$ for all $\omega \in (0, \omega_0)$, (the endpoint position is "approximately" equal to the input trajectory vector, e), the value of the contact force, f , within the bandwidth of the system ($0, \omega_0$) can be approximated by equation 31:

$$f_\infty \approx (S+H)^{-1}r \quad \text{for all } \omega \in (0, \omega_0) \quad (31)$$

By knowing S and choosing H , one can shape the contact force. The value of $(S+H)$ within $(0, \omega_0)$ is the designer's choice and, depending on the task, it can have various values in different directions (2,3). A large value for $(S+H)$ within $(0, \omega_0)$ develops a compliant system while a small $(S+H)$ generates a stiff system. If H is chosen such that $(S+H)$ is "large" in the singular value sense at high frequencies, then the contact force in response to high frequency components of r will be small. If H is chosen to guarantee the compliance in the system according to equation 29, then it must also satisfy the stability condition. It can be shown that the stability criterion for interaction with a very rigid environment is given by inequality 32:

$$\sigma_{max}(H) < \frac{1}{\sigma_{max}(S^{-1}G)} \quad \text{for all } \omega \in (0, \infty) \quad (32)$$

It is clear that if the environment is very rigid, then one must choose a very small H to satisfy the stability of the system when S is "small". (A good positioning system has "small" S). Since $G \approx I_n$ for all $\omega \in (0, \omega_0)$, the bound for H , for a rigid environment and a "small" stiffness, is given by 33.

$$\sigma_{max}(H) < \sigma_{min}(S) \quad \text{for all } \omega \in (0, \omega_0) \quad (33)$$

If S is zero, then no H can be obtained to stabilize the system. To stabilize the system of the very rigid environment and the robot, there must be a minimum compliancy in the robot. Direct drive manipulators, because of the elimination of the transmission systems, often have large S . This allows for a wider stability range in constrained manipulation.

We conclude that for stability of the environment and the robot taken as a whole, there must be some initial compliancy either in the robot or in the environment. The initial compliancy in the robot can be obtained by a non-zero sensitivity function or a passive compliant element such as an RCC. Practitioners always observed that the system of a robot

and a stiff environment can always be stabilized when a compliant element (e.g. piece of rubber or an RCC) is installed between the robot and environment. One can also stabilize the system of robot and environment by increasing the robot sensitivity function. In many commercial manipulators the sensitivity of the robot manipulators can be increased by decreasing the gain of each actuator positioning loop. This also results in a narrower bandwidth (slow response in the unconstrained maneuvering) for the robot positioning system.

8. Examples

Linear Example: Consider a one degree of freedom robot with G and S in equation 1 given as:

$$G(s) = \frac{1}{(s/6+1)(s/10+1)(s/200+1)(s/250+1)(s/300+1)}$$

$$S(s) = \frac{.05}{(s/5+1)(s/9+1)}$$

The system has a good positioning capability (small gain for S and unity gain for G at DC). The poles that are located at -250 and -300 show the high frequency modes in the robot. The stability of this system when it is in contact with various environment dynamics is analyzed. We assume E is constant and has the value of 10 for all frequency ranges. If we consider H as a constant gain, then inequality 27 yields that for $H < 0.14$ the value of $|GH|$ is always smaller than $|S+1/E|$ for all $\omega \in (0, \infty)$. Figure 7 shows the plots of $|GH|$ and $|S+1/E|$ for three values of H . For $H=0.08$ the system is stable with the closed loop poles located at $(-301.59, -244.81, -204.27, -9.25, -5.35, -7.37 \pm 8.4j)$ while $H=2.6$ results in unstable system with the closed loop poles located at $(-324.9, -221.31 \pm 63.52j, 0.78 \pm 37.82j, -9.01, -5.02)$. Note that the stability condition derived with inequality 27 is a sufficient condition for stability; many compensators can be found to stabilize the system without satisfying inequality 27. Figure 7 shows an example ($H=1.5$) that does not satisfy inequality 27 however the system is stable with closed loop poles at $(-317.67, -221.66 \pm 49.06j, -2.48 \pm 29.9j, -9.02, -5.03)$. If one uses root locus for stability analysis, for $H(2.32)$ all the closed loop poles will be in the left half plane. Once a constant value for stabilizing H established, one can choose a dynamic compensator to filter out the high frequency noise in the force measurements:

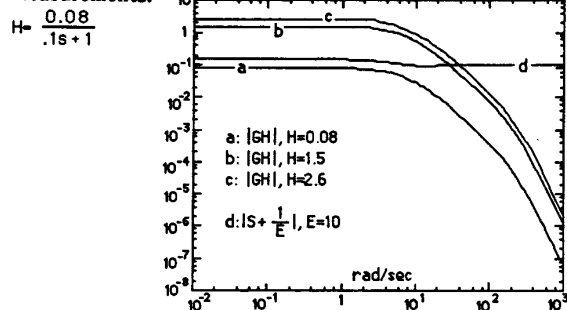


Figure 7: $|S+1/E|$ and GH for soft environment.

For a stiff environment ($E=1000$), when H is chosen as a constant gain, then inequality 27 yields that for $H < 0.01$ the magnitude of $|GH|$ is always smaller than $|S+1/E|$ for all $\omega \in (0, \infty)$. Figure 8 shows the plot of $|GH|$ and $|S+1/E|$ for three values of H . For $H=0.006$ the system is stable with the closed loop poles located at $(-309.03, -222.59 \pm 26.86j, -5.04 \pm 50.47j, -9.81, -5.88)$ while $H=0.03$ results in unstable system with the closed loop poles located at $(-326.74, -220.61 \pm 66.52j, 1.51 \pm 59.71j, -9.46, -5.60)$. Figure 8 also shows an example ($H=0.015$) which does not satisfy inequality 27 however the system is stable with closed loop poles at $(-317.41, -221.23 \pm 48.02j, -2.37 \pm 54.40j, -9.63, -5.75)$. If one uses root locus for exact stability analysis, for

$H \leq 0.023$ all the closed loop poles will be in the left half plane. Comparison between the stability condition for stiff and soft environments, shows that the soft environment yields a wider stability range.

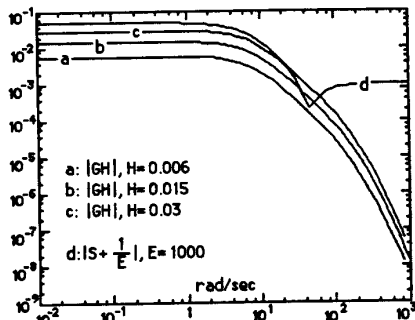


Figure 8: $|S+1/E|$ and GH for stiff environment.

Nonlinear Example: Consider a one degree of freedom robot with G and S in equation 1 given as:
 $G: e \rightarrow x$, such that $\ddot{x} + 9\dot{x} + 26x + 24(x+x^3) = e$ (note that $x=y$)
 $S=0$, (A non-direct drive robot with large transmission ratio results in a small sensitivity; commonly called stiff system)
 The environment dynamics is such that $f=p(x+x^3)$ where p is a constant. Since $S=0$, mapping $V:e \rightarrow f$ (defined by equation 15) is the solution of mapping G and $f=p(x+x^3)$. Also assume that the following structure has been proposed for compensator H to filter out the high frequency noise in measurement of the contact forces.

$$H = \frac{k}{s+1} \text{ where } k \text{ is the design parameter.}$$

Satisfaction of inequality 19, ($\alpha_4 \alpha_5 < 1$ in L_∞ sense), is the sufficient condition for stability of the system. α_4 and α_5 are the gains of operators V and H defined by inequalities 16 and 18 (Figure 5). We choose a unit step function for the input command, r, then we look for a k such that $\alpha_4 \alpha_5 < 1$. To calculate α_4 , $|f|$ is plotted versus $|e|$ in Figure 9 for two cases, $k=1$ and $k=20$, when $p=10$. By inspection of Figure 9, one can find that $\alpha_4 = 0.4707$ is the smallest tangent that allows $|f| = \alpha_4 |e|$ stands above all the possible values of $|f|$ for $k=1$. Figure 10 gives information about the size of α_5 . By inspection of Figure 11, $\alpha_5 = 1.0153$ is the smallest tangent that allows line $|z| = \alpha_5 |f|$ is above all the possible values of $|z|$ when $k=1$. Since $\alpha_4 \alpha_5 = 0.4779 < 1$, therefore the system is stable when the input command is a unit step function and $k=1$. Figure 11 shows the endpoint position, x, when the robot is in contact with an environment ($p=10$) and the input command, r, is unit step function. When $k=20$, the simulation results in unstable system. By inspection of Figure 9 and 10, the values for α_4 and α_5 that bound $|f|$ and $|z|$ when $k=20$ are 6.0993 and 187.887 respectively which results in $\alpha_4 \alpha_5 > 1$.

When $p=500$ (stiff environment in comparison with $p=10$), selection of $k=0.03$, results in $\alpha_4 = 25.75$, $\alpha_5 = 0.0318$ from Figures 12 and 13. This selection results in $\alpha_4 \alpha_5 = 0.819 < 1$ which is the sufficient condition for stability when r is unit step input and $k=0.03$. When $k=0.3$, the simulation results in unstable system. From Figures 12 and 13, $\alpha_4 = 870.3$, $\alpha_5 = 3.957$ which results in $\alpha_4 \alpha_5 > 1$. Figure 14 shows the simulation results.

9. Summary and Conclusion

A new controller architecture for compliance control has been investigated using unstructured models for dynamic behavior of robot manipulators and environment. This unified approach of modeling robot and environment dynamics is

expressed in terms of sensitivity functions. The control approach allows not only for tracking the input-command vector, but also for compliance in the constrained maneuverings. A bound for the global stability of the manipulator and environment has been derived. For stability of the environment and the robot taken as a whole, there must be some initial compliancy either in the robot or in the environment. The initial compliancy in the robot can be obtained by a non-zero sensitivity function for the positioning controller or a passive compliant element such as an RCC.

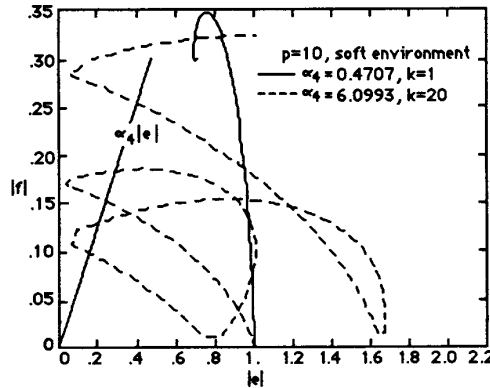


Figure 9: Calculation of gain of V.

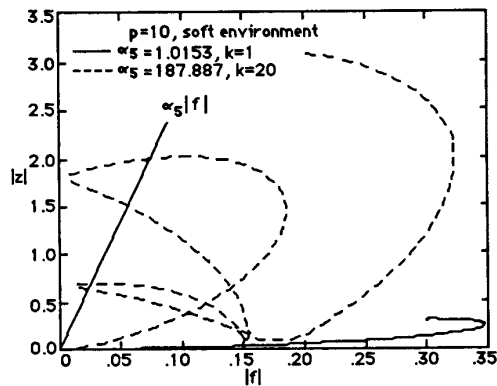


Figure 10: Calculation of gain of H.

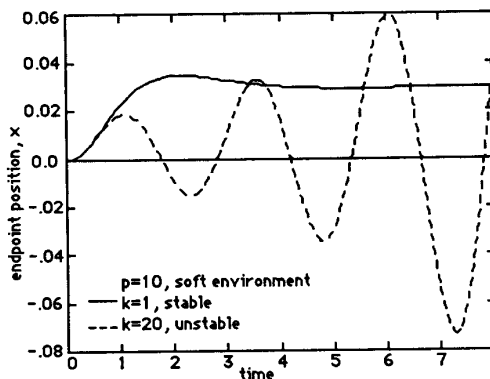


Figure 11: The endpoint position, x.

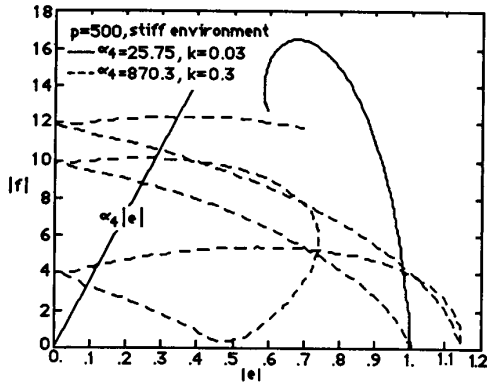


Figure 12: Calculation of Gain of V.

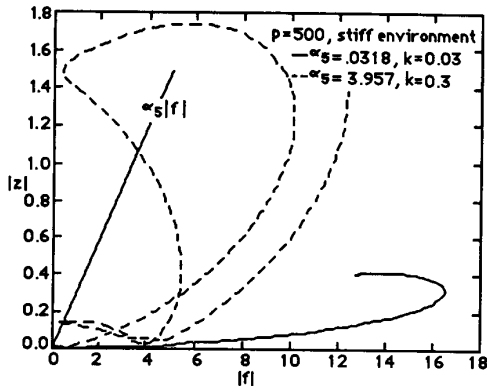


Figure 13: Calculation of Gain of H.

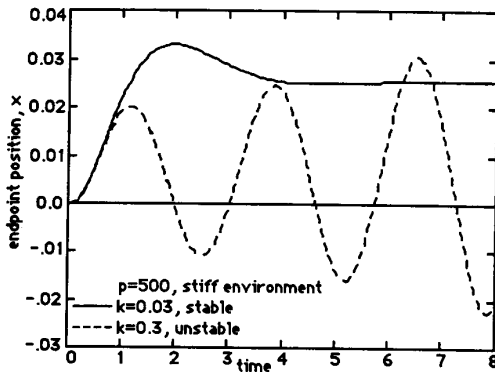


Figure 14: The Endpoint Position, x.

Appendix A

The following inequalities are true when $p=2$ and H and V are linear operators.

$$\|H(V(e))\|_p < \nu \|V(e)\|_p \quad (A1)$$

$$\|V(e)\|_p < \mu \|e\|_p \quad (A2)$$

where:

$\mu = \sigma_{\max}(Q)$, and Q is the matrix whose ij th entry is given by $(Q)_{ij} = \sup_{\omega} |(Q)_{ij}|$,

$\nu = \sigma_{\max}(R)$, and R is the matrix whose ij th entry is given by

$$(R)_{ij} = \sup_{\omega} |(R)_{ij}|$$

Substituting inequality A2 in A1:

$$\|HV(e)\|_p < \mu \nu \|e\|_p \quad (A3)$$

According to the stability condition, to guarantee the closed loop stability $\mu \nu < 1$ or:

$$\nu < \frac{1}{\mu} \quad (A4)$$

Note that the followings are true:

$$\sigma_{\max}(V) < \mu \quad \text{for all } \omega \in [0, \infty) \quad (A5)$$

$$\sigma_{\max}(H) < \nu \quad \text{for all } \omega \in [0, \infty) \quad (A6)$$

Substituting A5 and A6 into inequality A4 which guarantees the stability of the system, the following inequality is obtained:

$$\sigma_{\max}(H) < \frac{1}{\sigma_{\max}(V)} \quad \text{for all } \omega \in [0, \infty) \quad (A7)$$

$$\sigma_{\max}(H) < \frac{1}{\sigma_{\max}(E(I_n + SE)^{-1}G)} \quad \text{for all } \omega \in [0, \infty) \quad (A8)$$

Inequality A8 is identical to inequality 26. This shows that the linear condition for stability given by the multivariable Nyquist Criterion is a subset of the general condition given by the Small Gain Theorem.

References

- 1) Hogan, N., "Impedance Control, ASME Journal of Dynamic Systems, Measurement, and Control, 1985.
- 2) Kazerooni, H., Houpt, P. K., "On The Loop Transfer Recovery", Int. J. of Control, V.43, N.3, March 1986a.
- 3) Kazerooni, H. "Fundamentals of Robust Compliant Motion for Manipulators", IEEE J. of Robotics and Automation, N2, V2, June 1986b.
- 4) Kazerooni, H. "A Design Method for Robust Compliant Motion of Manipulators", IEEE Journal of Robotics and Automation, N2, V2, June 1986c.
- 5) Kazerooni, "An Approach to Automated Deburring by Robot Manipulators", ASME Journal of Dynamic Systems, Measurements and Control, December 1986d.
- 6) Kazerooni, H., "On the Stability of the Robot Compliant Motion Control", CDC 87, Los Angeles, December 1987.
- 7) Kazerooni, H., Guo, J., "Design and Construction of an Active End-Effector", IEEE International Conference on Robotics and Automation, Raleigh, North Carolina, April 1987, and also IEEE J. of Robotics and Automation.
- 8) Lancaster, P., Lambda-Matrices and Vibrating Systems. Pergamon Press, 1966.
- 9) Lehtomaki, N. A., "Robustness Results in Linear-Quadratic Gaussian Based Multivariable Control Designs", IEEE Trans. on Automatic Control, Feb., 1981.
- 10) Mason, M. T., "Compliance and Force Control", IEEE Tran. on Systems, Man, and Cybernetics June, 1981.
- 11) Paul, R. P. C., Shimano, B., "Compliance and Control", ACC, San Francisco, 1976.
- 12) Raibert, M. H., Craig, J. J., "Hybrid Position/Force Control of Manipulators", ASME Journal of Dynamic Systems, Measurement, and Control, June, 1981.
- 13) Salisbury, K. J., "Active Stiffness Control of Manipulator in Cartesian Coordinates", CDC, 1980.
- 14) Slotine, J. J., "The robust Control of of Robot Manipulators", The int. J. of Robotics Research, V4, 1985.
- 15) Vidyasagar, M., "Nonlinear Systems Analysis", Prentice-Hall, 1978.
- 16) Vidyasagar, M., Desoer, U. A., "Feedback Systems: Input-Output Properties", Academic Press, 1975.
- 17) Vidyasagar, M., Spong, M. W., "Robust Nonlinear Control of Robot Manipulators", CDC, December 1985.
- 18) Whitney, D.E., "Force-Feedback Control of Manipulator Fine Motions", ASME Journal of Dynamic Systems, Measurement, and Control :91-97, June, 1977.